Articles

Binding of α-Actinin to Titin: Implications for Z-Disk Assembly

R. Andrew Atkinson,[‡] Catherine Joseph,[‡] Fabrizio Dal Piaz,[§] Leyla Birolo,[||] Gunter Stier,[⊥] Piero Pucci,[§] and Annalisa Pastore*,[‡]

Division of Molecular Structure, National Institute for Medical Research, The Ridgeway, Mill Hill, London, United Kingdom, Dipartimento di Chimica Organica e Biologica, Università di Napoli Federico II and Centro Internazionale Servizi di Spettrometria di Massa, CNR−Università di Napoli Federico II, Napoli, Italy, Dipartimento di Chimica Organica e Biologica, Università di Napoli Federico II, Napoli, Italy, and European Molecular Biology Laboratory, Meyerhofstrasse 1, Heidelberg, Germany

Received August 12, 1999; Revised Manuscript Received January 25, 2000

ABSTRACT: Titin is an exceptionally large protein (M.Wt. ∼3 MDa) that spans half the sarcomere in muscle, from the Z-disk to the M-line. In the Z-disk, it interacts with α-actinin homodimers that are a principal component of the Z-filaments linking actin filaments. The interaction between titin and α-actinin involves repeating ∼45 amino acid sequences (Z-repeats) near the N-terminus of titin and the C-lobe of the C-terminal calmodulin-like domain of α-actinin. The conformation of Z-repeat 7 (ZR7) of titin when complexed with the 73-amino acid C-terminal portion of α-actinin (EF34) was studied by heteronuclear NMR spectroscopy using ^{15}N-labeling of ZR7 and found to be helical over a stretch of 18 residues. Complex formation resulted in the protection of one site of preferential cleavage of EF34 at Phe14-Leu17, as determined by limited proteolysis experiments coupled to mass spectrometry measurements. Intermolecular NOEs show Val16 of ZR7 to be positioned close in space to the backbone of EF34 around Phe14. These observations suggest that the mode of binding of ZR7 to EF34 is similar to that of troponin I to troponin C and of peptide C20W to calmodulin. These complexes would appear to represent a general alternative binding mode of calmodulin-like domains to target peptides.

Titin (also known as connectin) is an exceptionally large protein of M.Wt. ∼3 MDa (*1*, *2*), found in mammalian skeletal and cardiac muscle (for reviews, see refs *3*−*7*). A single molecule of titin spans half the sarcomere from the Z-disk to the M-line. Along its length, titin performs a range of functions and probably acts as a "molecular ruler" (*8*), controlling the length of the resting sarcomere. The sequence of titin shows it to be composed of a large number of smaller domains or modules, mostly belonging to the fibronectin type III and immunoglobulin superfamilies, termed type I and type II, respectively (*9*). The organization of these modules may be related to the varying functions performed along the length of the molecule. Thus, for example, titin in the A-band is composed of a specific pattern of repeating sequences of type I and type II modules, while in the I-band, only type II modules are found, arranged in tandem (*10*). Differing isoforms of titin are found in other tissues where they are associated with cytoskeletal structures (*11*). In *Drosophila*, a titin isoform is implicated in maintaining the structure of the chromosome (*12*).

* National Institute for Medical Research, The Ridgeway, Mill Hill, London NW7 1AA, U.K. Tel: (44) 0208 959 3666. Fax: (44) 0208 906 4477. E-mail: apastor@nimr.mrc.ac.uk.

[‡] National Institute for Medical Research.

[§] CNR−Università di Napoli Federico II.

[||] Università di Napoli Federico II.

[⊥] European Molecular Biology Laboratory.

Titin binds to α-actinin (*13*−*15*), a protein from the spectrin gene superfamily that also includes the actin-binding proteins spectrin and dystrophin (*16*). α-Actinin is a major component of the Z-disk, where actin filaments are anchored (see ref *17* and references therein), and is also found in nonmuscular cells, where it interacts with a cellular isoform of titin involved in the cytosketelal structure (*11*). The sequence of the C-terminal portion of α-actinin contains a calmodulin-like domain composed of four noncanonical EF-hand motifs that have no ability to bind calcium (*16*). This C-terminal domain of α-actinin is involved in binding to titin (*13*, *15*) but, within the domain, only the 73 C-terminal amino acids, corresponding to the second pair of noncanonical EF-hands, are necessary and sufficient for the interaction (*14*). Fragments lacking either this entire portion or the C-terminal 21 amino acids do not bind to titin (*14*).

α-Actinin interacts with titin in the region localized in the Z-disk (*15*, *18*), in particular with the repeating 45−50 amino acid sequence motifs near the N-terminus of titin, termed Z-repeats (*19*). The number of Z-repeats in titin varies between species and between muscle types, the latter variation arising from alternative splicing and being correlated with the thickness of the Z-disk (*19*). The interaction of α-actinin with the C-terminal Z-repeat is most readily detected, but the protein does bind to other repeats (*15*). Only half of the last titin Z-repeat is required for binding to

10.1021/bi991891u CCC: $19.00
Published on Web 03/28/2000

α-actinin (*14*).

While information on structure and stability is available for a number of modules from titin, representing the molecule at different points along its length (*20*−*25*), little is known about the Z-repeats. Similarly, α-actinin has not been characterized at a detailed structural level. The interaction of the C-terminal EF-hand (EF34[1]) of α-actinin from skeletal muscle with the seventh and last Z-repeat of titin (ZR7) is investigated here, by limited proteolysis in combination with mass spectrometric methods and by heteronuclear nuclear magnetic resonance spectroscopy. While related complexes have been studied by NMR (*26*, *27*), this is the first instance in which uniform labeling of the peptide target is used, allowing direct characterization of the bound peptide. Characterization of the complex allows the conformation of the binding site within the Z-repeat to be described at an atomic level and comparison with the binding of calmodulin and troponin C to target peptides to be made. The implications for the structure of the Z-disk are discussed in light of recent models.

EXPERIMENTAL PROCEDURES

Sample Preparation. Samples were prepared as described in detail elsewhere (manuscript in preparation). Briefly, the constructs were produced as fusion proteins with a His-tagged GST separated by a TEV protease cleavage site expressed in *Escherichia coli*. ^{15}N-labeled samples were produced growing the bacteria in minimal medium using $^{15}NH_4Cl$ as sole source of nitrogen. Samples were ∼0.7 mM in 20 mM phosphate buffer at pH 6.6.

NMR Spectroscopy. All NMR spectra were recorded at 500 and 600 MHz (^{1}H frequency) and at 27 °C on Varian Unity Plus 500 and 600 spectrometers. Two-dimensional ^{1}H NOESY (*28*) and TOCSY (*29*, *30*) spectra were acquired at 500 MHz with mixing times of 150 ms and 60 ms, respectively, and using a WATERGATE (*31*, *32*) sequence prior to acquisition to suppress the water signal. A two-dimensional ^{15}N-^{1}H HSQC (*33*) spectrum, with WATERGATE sequence, was acquired at 600 MHz with spectral widths of 6000 Hz (^{1}H) and 1400 Hz (^{15}N), respectively. A total of 256 t_1 increments were acquired with an acquisition time of 0.15 s, during which the ^{15}N nuclei were decoupled using a GARP sequence (*34*).

A three-dimensional ^{15}N-^{1}H NOESY−HSQC experiment, an HSQC version of the NOESY−HMQC (*35*, *36*), was acquired at 600 MHz with spectral widths as above, a mixing time of 80 ms, 100 increments in the indirect ^{1}H dimension and 24 increments for the ^{15}N dimension. Three-dimensional ^{15}N-^{1}H TOCSY−HSQC (*35*), HNHA (*37*), and HNHB (*38*) experiments were acquired at 500 MHz with spectral widths of 6000 or 5800 Hz (^{1}H) and 1200 Hz (^{15}N), except in the HNHA experiment where the spectral width was reduced to 2650 Hz (5.3 ppm) in the indirect ^{1}H dimension. For the TOCSY−HSQC and HNHA experiments, 27 increments were acquired for the ^{15}N dimension while 128 and 96 increments were acquired for the indirect ^{1}H dimension in the TOCSY−HSQC and HNHA experiments, respectively. In the HNHB experiment, 24 increments were acquired for the ^{15}N dimension and 120 in the indirect ^{1}H dimension. Acquisition times of 0.15 s were used throughout, again with decoupling of the ^{15}N nuclei using a GARP sequence. The mixing time for the TOCSY−HSQC was 70 ms. A further set of ^{15}N-^{1}H HSQC spectra were recorded at 500 MHz (^{1}H frequency), as described above, at temperatures of 5 °C, 10 °C, 15 °C, 20 °C, 25 °C, and 30 °C. The slopes of the plots of the chemical shifts of the amide HN resonances versus temperature were determined by linear regression using Matlab (The MathWorks Inc., Natick, MA).

All spectra were processed using nmrPipe (*39*) and analyzed using XEASY (*40*). Typically, the acquisition dimension was multiplied by a Gaussian function, and other dimensions with a 90°-shifted sine-bell function. All dimensions were zero-filled at least to the next power of two. The volumes of HN and HN−Hα peaks in the HNHA spectrum were integrated in XEASY using the elliptical interactive integration mode and the ratio of the peaks used to calculate $^3J_{HNH\alpha}$ coupling constants (*37*).

Limited Proteolysis Experiments. EF34 and ZR7 were each incubated with trypsin, chymotrypsin, subtilisin, and endoprotease V8 using enzyme-to-substrate ratios ranging from 1:6000 to 1:100 (w/w). The extent of each reaction was monitored on a time-course by sampling the incubation mixture at different time intervals. Proteolytic fragments were fractionated by reverse-phase HPLC on a Phenomenex Jupiter C18 column with a linear gradient from 5% to 50% of acetonitrile in 0.1% TFA over 40 min. Elution was monitored at 220 and 280 nm. Fractions were collected and identified by ESMS.

For experiments on the complex formed by EF34 and ZR7, EF34 was preincubated with a 3-fold excess of ZR7, in phosphate buffer at pH 7, prior to protease addition. In this case, enzyme-to-substrate ratios ranging from 1:2500 to 1:50 were used.

Gel Filtration. The isolated proteins, EF34 and ZR7, and the complex formed by association of the two proteins were analyzed by gel filtration chromatography. For each hydrodynamic measurement, 50 μL of the samples, 50 μM in 10 mM phosphate buffer at pH 7, 0.15 M NaCl, were loaded on a Superdex 75 PC (0.32 × 30 cm) gel filtration column installed on a Smart System (Pharmacia, Uppsala, Sweden) and isocratically eluted in 10 mM phosphate buffer at pH 7, 0.15 M NaCl. All experiments were carried out at 25 °C at a flow rate of 40 μL min^{-1}. The column was calibrated in the same conditions with the following proteins of known molecular mass: bovine serum albumin (66 000 Da), white egg albumin (45 000 Da), carbonic anhydrase (29 000 Da), α-lactalbumin (14200 Da), cytochrome *c* (12 400 Da).

Mass Spectrometry. Protein samples and proteolytic fragments were analyzed by ESMS using a Bio-Q triple quadrupole mass spectrometer (Micromass, Manchester, U.K.), equipped with an electrospray ion source. Samples were injected into the ion source (kept at 80 °C) via an injection loop at a flow rate of 10 μL min^{-1}. Data were acquired and elaborated using the MASSLYNX program

[1] Abbreviations: EF34, C-terminal 73 residues of α-actinin; ZR7, seventh Z-repeat of titin (the nomenclature for the Z-repeats varies among authors—here the least ambiguous system is adopted); GST, glutathione S-transferase; NOESY, nuclear Overhauser enhancement spectroscopy; TOCSY, total correlation spectroscopy; HSQC, heteronuclear single quantum correlation; ESMS, electrospray mass spectrometry; HPLC, high performance liquid chromatography; TFA, trifluoroacetic acid; TnC, troponin C; TnI, troponin I; TnI_{1-47}, a peptide spanning the sequence 1−47 of TnI. Standard three- and one-letter abbreviations are used for the amino acids.

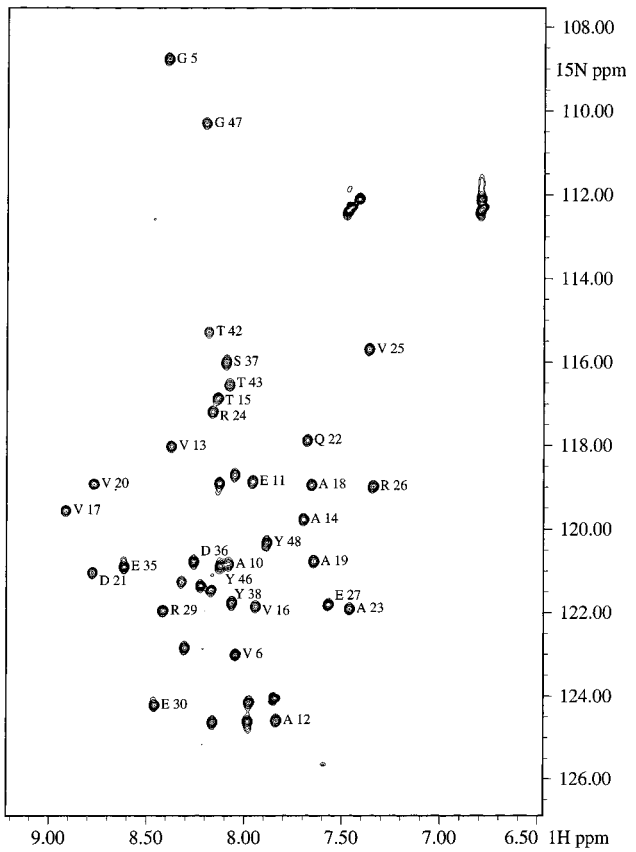

FIGURE 1: ^{15}N-^{1}H HSQC spectrum of EF34-ZR7 complex in which ZR7 is ^{15}N-labeled. The cross-peaks of assigned ZR7 residues are labeled, numbered as follows:

GA MGKVGVGKKA EAVATVVAAV DQARVREPRE
10 20 30
PGLPEDSYAQ QTTLEYGYKE H
40 50

The sequence of EF34 is as follows, with expected helical regions underlined (based on the alignment of α-actinin with other members of the spectrin superfamily (*50*):

MADTDTAEQV IASFRILASD KPYILAEELR RELPPDQAQY
10 20 30 40
CIKRMPAYSG PGSVPGALDY AAFSSALYGE SDL
50 60 70

(Micromass, Manchester, U.K.). Mass calibration was performed by means of multiply charged ions from a separate injection of horse heart myoglobin (Sigma, average molecular mass: 16 951.5 Da). All masses are reported as average values.

Molecular Modeling. Multiple sequence alignment was achieved by CLUSTALX or, when necessary, manually using the GDE sequence editor (S. Smith, Harvard University) and COLORMASK (J. Thompson, EMBL Heidelberg). A three-dimensional model of the EF34-ZR7 complex was generated using the BLDPSQ option in WHATIF (*41*), with the coordinates of the TnC-TnI$_{1-47}$ complex (*42*) serving as a template. No attempt to model insertion/deletions in EF34 was made.

RESULTS

Helical Propensity of ZR7. One-third of the amino acids of ZR7 are hydrophobic while positively and negatively charged side chains are present in almost equal numbers (Figure 1 legend). The presence, however, of a small number of prolines in the center of the sequence and a concentration of alanine and valine residues nearer the N-terminus are its most striking features. The helical propensity for ZR7 in aqueous solution at 5 °C, predicted by AGADIR (*43*), is very low (data not shown). This is in agreement with the "random coil" NMR spectra recorded for ZR7, free in solution (see below). Slightly higher values, rising to just above 3%, are predicted for the N-terminal region, preceding the set of proline residues.

To compare with relevant systems, known to adopt a helical conformation when complexed, similar calculations were performed for a peptide from rabbit troponin I (TnI$_{1-47}$), which binds to TnC (*42*), and for a sequence from smooth muscle myosin light chain kinase (ARRKWQKTGHAVRAIGRLSS) that binds to calcium-loaded calmodulin (*44*). The helical propensity for the former rises to just 5% while for the latter it does not reach 1%, reflecting the fact that a predisposition of the peptide to form helices when isolated in solution is not required for adopting such a structure when complexed (*45*).

NMR Spectroscopy of EF34-^{15}N-ZR7. Uniform ^{15}N-labeling of ZR7 allowed the peptide to be observed directly in the complex. The spectra of ^{15}N-ZR7 free in solution are those of an unstructured polypeptide with resonances at "random coil" positions (data not shown). The spectra of the EF34-^{15}N-ZR7 complex show far greater dispersion of resonances. In particular, shifted methyl groups are found as far upfield as 0.12 ppm (Figure 2) and HN resonances as far downfield as 9.75 ppm. The ^{15}N-^{1}H HSQC spectrum (Figure 1) of the EF34-^{15}N-ZR7 complex allowed identification of the ^{15}N and HN resonances of the labeled moiety. Many of these resonances were clearly shifted from "random coil" positions. The ^{15}N-^{1}HN strips from the TOCSY−HSQC spectrum gave indications as to the amino acid types of the spin systems.

The ^{15}N-^{1}HN strips from the NOESY−HSQC spectrum could immediately be divided into two sets. A large number showed some nuclear Overhauser effects from the HN resonance to aliphatic protons, shown by the TOCSY−HSQC spectrum to be in large part intraresidue NOEs, no cross-peaks to other HN resonances, and a strong exchange peak at the water frequency. The remaining 18 strips (Figure 2) showed NOEs to other HN resonances and little or no exchange with water. The temperature coefficients for these HN resonances are lower than "random coil" values throughout this region, indicating protection from exchange with water through hydrogen bonding and/or inaccessibility to solvent. Values for all other residues, assigned and unassigned, lie closer to the values for exposed peptide groups. These qualitative observations indicate that a core set of 18 residues of ^{15}N-ZR7, unstructured when free in solution, becomes structured on binding to EF34, while the remaining sequence is unstructured.

Assignment of the resonances of the ^{15}N, HN, Hα nuclei and some side chain protons could be achieved readily for the set of 18 strips from analysis of HNHA, HNHB, TOCSY−HSQC, and NOESY−HSQC spectra (Table 1, chemical shift and coupling constant data deposited with the BioMagResBank (http://www.bmrb.wisc.edu) under accession number 4454). These correspond, unequivocally, to residues from Ala10 to Glu27 of the ZR7 sequence (for full sequence, see Figure 1 legend or Figure 3). The NOEs characteristic of α-helical structure and the $^{3}J_{HNH\alpha}$ coupling

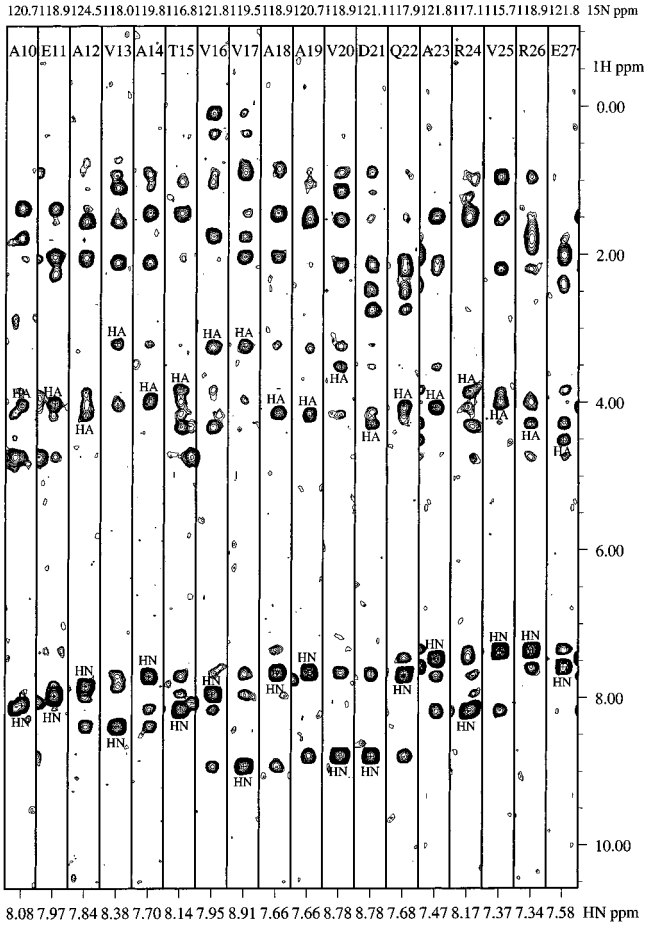

FIGURE 2: ^{15}N-^{1}H strips taken from the NOESY−HSQC spectrum of EF34-^{15}N-ZR7 for residues Ala10-Glu27. Diagonal peaks (N−HN−HN) and intraresidue cross-peaks to the Hα resonance (N−HN−Hα) are labeled. The spectrum was recorded at 600 MHz (^{1}H frequency) and 27 °C.

constants for this portion are given in Figure 3, together with secondary chemical shifts. The $H\alpha_i-HN_{i+3}$ NOE is not observed for Thr15, suggesting a possible disruption of the helix at this point. A NOE between Thr15 Hγ and Ala19 HN supports this notion, although no discontinuity is observed in the other measured indicators. Intensity is observed in the homonuclear NOESY spectrum at the expected positions of $H\alpha_i-H\beta_{i+3}$ NOEs throughout the 18-residue segment, but must be treated with caution since the spectrum includes cross-peaks from both components of the complex.

For the remainder of the sequence, tentative assignments for only a small number of residues (Table 1) could be made due to a lack of NOEs and/or resonance overlap. Only two other $^{3}J_{HNH\alpha}$ coupling constants have values below 5 Hz. These correspond to Glu35 and Thr42 but are isolated and are not small enough to warrant particular attention.

Inspection of the homonuclear NOESY spectrum of the complex shows a number of intermolecular contacts. Of these, the most upfield-shifted resonances (0.35 and 0.12 ppm), assigned to the Hγ resonances of Val16 of ZR7 (Table 1), give cross-peaks to a set of downfield resonances. Assignment of the spectrum of EF34 in the complex (BioMagResBank accession number 4453) allows some of these resonances to be identified as those of the amide and aromatic protons of EF34 Phe14.

Limited Proteolysis Experiments. The interaction between EF34 and ZR7 was investigated by a strategy combining limited proteolysis with mass spectrometric analysis of the fragments generated (*46*, *47*). The rationale behind the approach is that the interface formed by the two proteins is shielded in the complex but should be accessible to proteases in the isolated molecules. Therefore, different proteolytic patterns are expected, depending on whether the digestion is carried out on the isolated components or on the complex, from which the interface regions can be inferred.

Limited proteolysis of isolated EF34 and ZR7 and of the EF34-ZR7 complex, by trypsin, chymotrypsin, subtilisin, and endoprotease V8, was performed under conditions appropriate to maintain the native conformation of each protein, to maximize the stability of the complex and to optimize the selectivity of the proteases (*48*, *49*). Gel filtration established that the complex was formed. Isolated EF34 eluted from the gel permeation column with an estimated molecular mass in good agreement with the expected value. The elution time of ZR7, however, was shorter than expected, confirming that the protein is unstructured in solution. The EF34-ZR7 complex eluted slightly before isolated EF34, and the chromatographic profile contained a second peak whose retention time matched that of isolated ZR7 (data not shown).

Proteolysis of Isolated EF34. The HPLC profiles of aliquots, taken from the incubation mixture after 15 and 30 min of tryptic digestion of isolated EF34, are shown in Figure 4a. Under the experimental conditions used, the protein remained largely undigested. Only a limited number of fragments were released from the protein molecule, showing that its native conformation is susceptible to proteolysis at a few very specific, and most probably flexible, sites. Preferential proteolytic cleavage sites within the EF34 structure were detected at Arg15, Arg31, and Lys43, inferred by the detection of sets of complementary peptides Met1-Arg15 and Ile16-Leu73, Met1-Arg31 and Glu32-Leu73, and Met1-Lys43 and Arg44-Leu73. These fragments were released almost simultaneously early in the process, indicating that the three sites display similar kinetics of hydrolysis (Figure 4a, panel A). At later stages of digestion, the primary fragments underwent further cleavage, leading to the formation of smaller fragments that accumulate as the hydrolysis time increases. These peptides were not considered in the identification of preferential cleavage sites since none were released from intact EF34 but were generated by subsequent digestion of larger fragments.

Similar results were obtained using endoprotease V8 and the enzymes with broad specificity, chymotrypsin and subtilisin. As an example, Figure 4b shows the HPLC time-course analysis for chymotrypsin digestion. Again, proteolysis occurred only at few, very specific sites within the EF34 structure. Only two complementary peptide pairs could be identified: Met1-Phe14 and Arg15-Leu73, and Met1-Tyr40 and Cys41-Leu73, identifying Phe14 and Tyr40 as preferential cleavage sites.

The combined results of the limited proteolysis experiments are summarized in Figure 5, from which a number of conclusions may be drawn. The native conformation of EF34 is rather resistant to proteolysis, as expected for a polypeptide chain adopting a defined tertiary structure. Preferential cleavage sites were located in three well-defined regions of the protein structure: segments Phe14-Leu17, Glu28-Arg31,

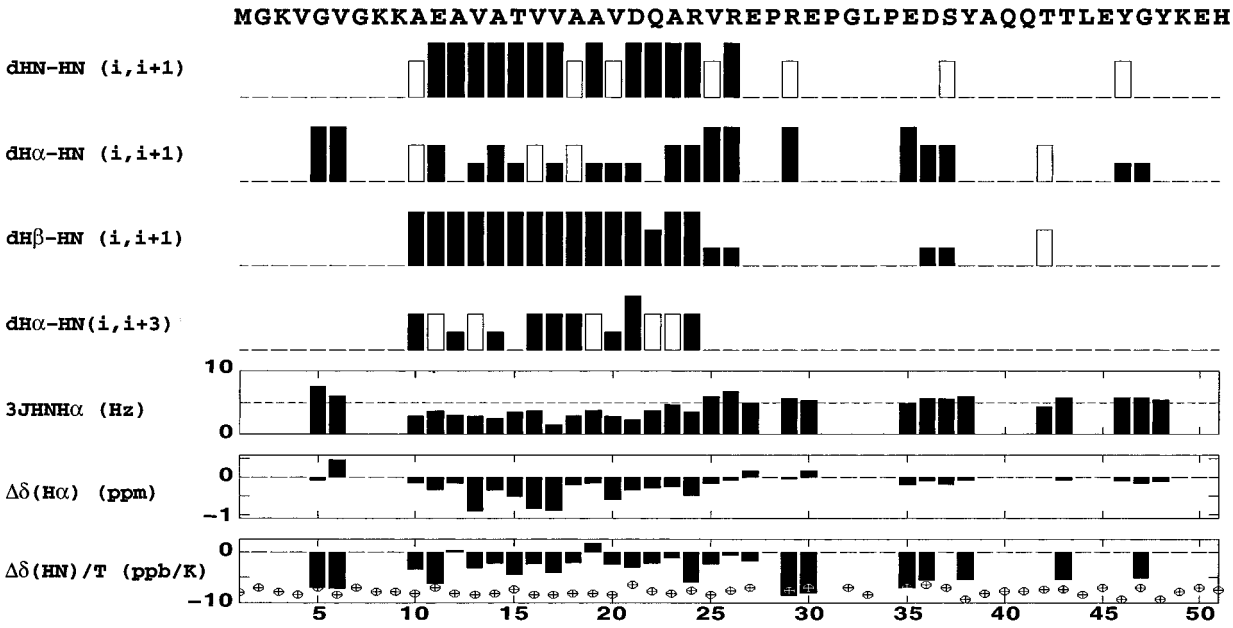

FIGURE 3: Summary of NMR data used for assignment and identification of secondary structure. The sequence is given along the top of the figure and numbering along the bottom. From top to bottom: (*i*−*iv*) The strength of sequential (*i*, *i+1*) and short-range (*i*, *i+3*) NOEs is indicated by the height of the filled bars. Open bars indicate residues for which the strength of the NOE could not be determined due to resonance overlap. (*v*) $^3J_{HNH\alpha}$ coupling constants determined from the HNHA experiment. Errors on the reported values are estimated to be ±0.2 Hz. (*vi*) Secondary chemical shift of Hα resonances from "random coil" values (*64*). (*vii*) Temperature coefficients for HN resonances (in ppb K^{-1}). "Random coil" values are indicated by ⊕ (*65*).

Table 1: ^{15}N and ^1H Resonance Assignments (in ppm) for ^{15}N-Labeled ZR7 Complexed to Unlabeled α-Actinin EF34[a]

residue	N	HN	Hα	Hβ	Hγ	Hδ
Gly5	108.72	8.39	3.89	–	–	–
Val6	123.04	8.04	4.60	1.56	0.88	–
Ala10	120.74	8.09	4.03	1.39	–	–
Glu11	118.94	7.96	4.02	2.05		–
Ala12	124.56	7.83	4.16	1.57	–	–
Val13	117.96	8.37	3.21	2.11	1.11, 0.92	–
Ala14	119.76	7.70	3.97	1.44	–	–
Thr15	116.83	8.14	3.83	4.33	1.03	–
Val16	121.91	7.94	3.28	1.77	0.35, 0.12	–
Val17	119.47	8.91	3.22	2.05	0.92, 0.84	–
Ala18	118.98	7.66	4.12	1.46	–	–
Ala19	120.91	7.65	4.16	1.54	–	–
Val20	118.97	8.77	3.52	2.14	1.17, 0.89	–
Asp21	120.95	8.78	4.29	2.75, 2.48	–	–
Gln22	117.89	7.68	4.06	2.23, 2.10	2.35	–
Ala23	121.94	7.46	4.07	1.49	–	–
Arg24	117.17	8.17	3.85	1.56		
Val25	115.70	7.36	3.97	2.21	0.96	–
Arg26	119.00	7.34	4.27	1.94, 1.79	1.63	
Glu27	121.89	7.57	4.53	2.03	2.38	–
Arg29	121.98	8.41	4.30	1.73, 1.64		
Glu30	124.19	8.45	4.53	2.00, 1.86	2.25	–
Glu35	120.92	8.61	4.14	2.00, 1.91	2.23	–
Asp36	120.81	8.26	4.55	2.61, 2.23	–	–
Ser37	116.03	8.09	4.29	3.73	–	–
Tyr38	121.68	8.06	4.47	3.05, 2.95	–	
Thr42	115.32	8.19	4.33	4.14	1.11	–
Thr43	116.43	8.08	4.28	4.16	1.11	–
Tyr46	120.87	8.12	4.46	2.95, 2.86	–	
Gly47	110.23	8.20	3.81	–	–	–
Tyr48	120.40	7.89	4.44	2.92	–	

[a] The sample is 0.7 mM in 20 mM phosphate buffer at pH 6.6, and spectra were recorded at 27 °C.

and Tyr40-Lys43. These regions should be considered to be exposed and flexible and might constitute loops connecting elements of secondary structure.

Proteolysis of Isolated ZR7. In contrast to isolated EF34, preferential cleavage sites are located at many points along the sequence of isolated ZR7 (Figure 5). The only regions showing resistance to the proteases were the segment Val25-Ala39 and the extreme C-terminal residues Tyr48-His51. The absence of proteolytic sites at the C-terminus was rather surprising since the segment Gln40-Tyr46 was cleaved at nearly all possible sites, indicating a region of high flexibility. In the remainder of the ZR7 sequence, the specific proteases trypsin and endoprotease V8 digested the protein essentially at all the anticipated cleavage sites with the exception of Arg26, Arg29, and Glu35. The two arginine residues are both involved in Arg-Glu peptide bonds that always show slower kinetics of hydrolysis. All three sites are located within a region containing three proline residues which might be responsible for some rigidity of this region, impairing protease action. The results suggest that ZR7 in solution is largely disordered, lacking any three-dimensional structure capable of limiting protease activity.

Proteolysis of EF34-ZR7 Complex. A higher enzyme-to-substrate ratio was needed to observe proteolysis for the EF34-ZR7 complex, reflecting greater resistance to protease action and suggesting a tightening of the EF34 structure on interaction with ZR7.

As an example, the HPLC time-course analysis of the complex digested with trypsin is shown in Figure 4c. The results of the digestions (Figure 5) show clear effects of the interaction with ZR7. A number of fragments were released from unbound ZR7, due to the large excess of the protein, free in solution. The release of complementary pairs of peptides Met1-Arg31 and Arg32-Leu73, and Met1-Lys43 and Arg44-Leu73 showed that EF34 was rapidly cleaved at Arg31 and Lys43. No further cleavage was observed even at long hydrolysis times. Comparison of these results with

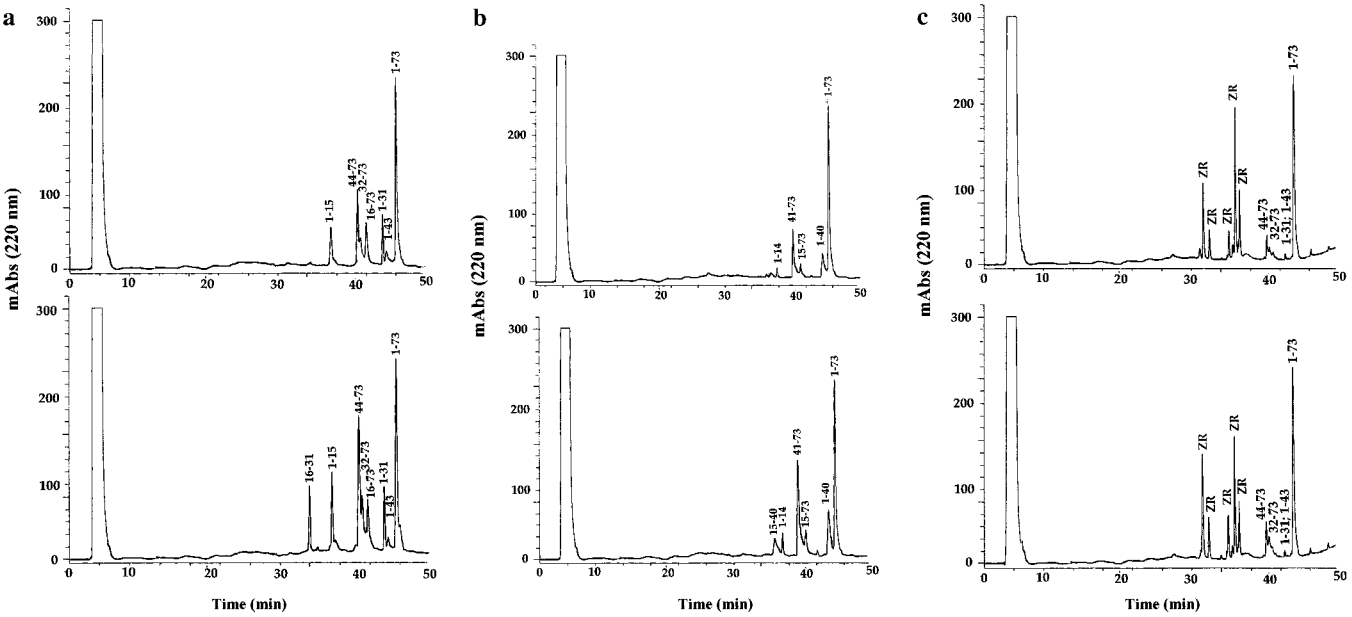

FIGURE 4: Results of limited proteolysis experiments on EF34 isolated and complexed with ZR7. HPLC chromatograms of the aliquots were taken from the incubation mixture after 15 min (upper panels) and 30 min (lower panels). Individual fractions were collected and analyzed by ESMS. (a) Time-course analysis of EF34 digested with trypsin at pH 7, 37 °C, using an enzyme-to-substrate ratio of 1:1000. (b) Time-course analysis of EF34 digested with chymotrypsin at pH 7, 37 °C, using an enzyme-to-substrate ratio of 1:6000. (c) Time-course analysis of the EF34-ZR7 complex digested with trypsin using an enzyme-to-substrate ratio of 1:2500. Peaks marked "ZR" correspond to ZR7 and its digestion products.

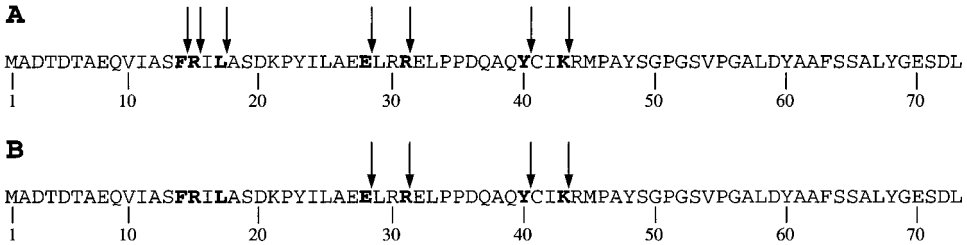

FIGURE 5: Location of preferential cleavage sites in EF34 (A) isolated and (B) complexed with ZR7.

those obtained for the isolated protein show that complex formation results in almost complete shielding of Arg15. The anticipated peptide fragments Met1-Arg15 and Ile16-Leu73, observed in the tryptic digestion of isolated EF34, could not be detected in the complex. Thus, following complex formation, EF34 still showed accessibility to proteases within the regions Glu28-Arg31 and Gln39-Leu43, whereas the segment Phe14-Leu17 seemed to be completely protected by the presence of ZR7.

Molecular Modeling. A qualitative model of the EF34-ZR7 complex was prepared as follows using the TnC/TnI_{1-47} complex as template.

The α-actinin C-terminal domain was aligned with the rabbit TnC and *Xenopus* calmodulin sequences (Figure 6a), as described by Travé et al. (*50*). No insertions/deletions are present in the sequences of TnC and calmodulin except for a three-residue insertion in TnC in the tethering helix which connects the two globular halves and therefore precedes the region of α-actinin studied in the present work. The sequence of EF34, however, contains two deletions and two insertions with respect to those of calmodulin and TnC. The insertions/deletions occur in both the EF-loops which must therefore be expected to adopt a conformation quite different from that of classical EF-hand proteins. This is in agreement with the fact that α-actinin EF34 is calcium-insensitive (*16*).

Alignment of TnI_{1-47} to the Z-repeats was achieved manually, since the sequences are too divergent, assuming that the contact observed between Val16 of ZR7 and EF34 Phe14 corresponds to that between Met21 of TnI_{1-47} with Phe99 of troponin C (Figure 6b). The alignment could be displaced by ±1 turn of the α-helix and still possibly account for the observed NOEs but nonetheless positions the ZR7 peptide such that the region of TnI_{1-47} with low accessible surface area (residues 9−29) corresponds to that observed to be protected in ZR7 by temperature coefficients (18 residues) and mass spectrometry.

Using these alignments of the two components, the side chains of the template structures were mutated into the corresponding side chains of the target sequences, and steric contacts were removed. The model so obtained is displayed in Figure 6c and compared with the template (Figure 6d). Val16 of ZR7 is buried in the interior of the complex and surrounded by hydrophobic residues of EF34.

DISCUSSION

The complex formed in solution between the C-terminal fragment of α-actinin EF34 and titin ZR7 causes the latter to adopt an α-helical structure, characterized in the NMR spectrum by small $^3J_{HNH\alpha}$ coupling constants, low temperature coefficients for HN resonances, weak cross-peaks from

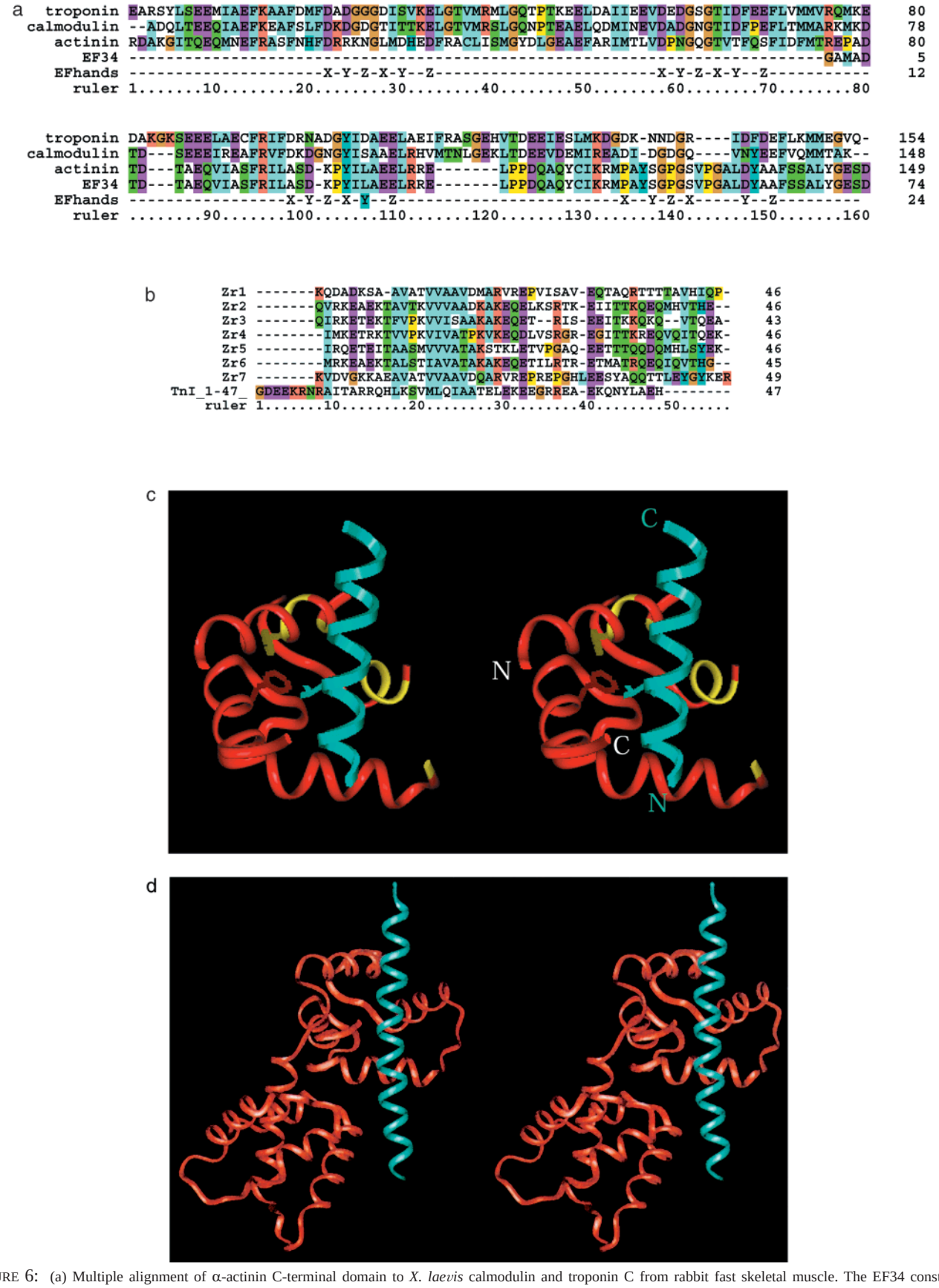

FIGURE 6: (a) Multiple alignment of α-actinin C-terminal domain to *X. laevis* calmodulin and troponin C from rabbit fast skeletal muscle. The EF34 construct (EF34) and the position of the four EF-hands (EFhands) are indicated. The sequences are color-coded according to amino acid properties. The figure was produced by CLUSTALX (*66*). (b) Multiple alignment of the human cardiac Z-repeats (*19*). The sequence used in the present paper is from rabbit and differs from the human by three amino acids all in the C-terminus and therefore outside the binding region. The sequence of TnI_{1-47} is also included and aligned to match Met21 with Val16 of ZR7 as suggested by experimental data. The color coding is the same as in (a). (c) Molecular model of the EF34-ZR7 complex based on the structure of TnC-TnI_{1-47} (*42*). ZR7 is represented by a green ribbon with the side chain of Val16 displayed. The backbone of EF34 is shown in red, except for the sites of preferential cleavage (in yellow). Discontinuities in the ribbon correspond to gaps in the alignment with TnC (see Figure 6a). The side-chain of Phe14 (in yellow) is displayed. (d) Structure of the complex of troponin C with TnI_{1-47} (*42*) in the same orientation as (c) but including the N-lobe of troponin C. TnC is shown in red and TnI_{1-47} in green.

HN resonances at the water frequency, and both sequential and short-range NOEs typical of an α-helix. The portion of the peptide so structured corresponds precisely to that mapped by Ohtsuka et al. (*14*) by yeast two-hybrid methods as the minimal sequence necessary and sufficient for binding to α-actinin. The information gained from the study of the structure of the EF34-ZR7 complex in solution is thus relevant for the interaction between the intact proteins, α-actinin and titin.

Clearly, little can be deduced about the structure of the Z-repeats within titin in the absence of α-actinin, but this is not a state that is of great importance, since titin and α-actinin co-localize during myofibrillogenesis (*51*, *52*). The sequence of ZR7 is highly hydrophobic, no fewer than 11 of the 18 residues being either alanine or valine. These residues are the least variable among any set of Z-repeats (*19*). The central region of ZR7 contains three prolines that are expected to disrupt the α-helical structure while the remainder of the sequence has no strong tendency for a particular secondary structure. The C-terminal portion of ZR7 is clearly not involved in the formation of the complex and, in agreement, is not required for binding to the C-terminal half of α-actinin (*14*). A truncated peptide should therefore be capable of binding to EF34 with a similar affinity.

The results of yeast two-hybrid studies (*15*) implied that the affinities of α-actinin for the various Z-repeats differed, with the highest affinity being for ZR7. In that case, the least variable residues might be thought to provide a binding motif, while the more variable residues control the affinities. The affinities for ZR1 and ZR7 are, in fact, comparable (manuscript in preparation), while there is weaker binding to the intervening Z-repeats (*18*). The importance of individual side-chains in the binding of ZR7 to α-actinin should become clearer when a full structure of the complex is available.

The observed intermolecular contacts observed between Val16 of ZR7 and EF34 Phe14 agree well with the protection observed in limited proteolysis experiments and comparison with the complexes of similar systems. Protection from proteolysis on formation of the complex was localized to Phe14, Arg15, and Leu17 of EF34. Although the EF-hands of α-actinin do not bind calcium ions (*16*), their interaction with the seventh Z-repeat of titin may be usefully compared with the complexes formed by the calcium-dependent EF-hand proteins calmodulin, with peptides from its target proteins (*53*, *54*), and TnC, with TnI (*55*, *56*).

The interactions of TnC with TnI (*42*) involve primarily the pair of EF-hands of the C-terminal regulatory domain of TnC. In contrast, the structure of the complex of calcium-loaded calmodulin with a peptide from myosin light-chain kinase (*26*, *44*) is seen to be compact, with the two pairs of EF-hands wrapping around the helical MLCK peptide. A comparison with calmodulin would, at first, appear rather difficult since the structures of several calmodulin/peptide complexes have been described in which the interaction is achieved by collapse of the two globular halves of the protein around the peptide. While this seems to be the most common mode of interaction, the formation of "dumbbell"-shaped complexes has also been described: the complex of calmodulin with a peptide from the regulatory domain of the catalytic subunit of phosphorylase kinase retains the extended dumbbell shape of uncomplexed calmodulin (*57*), as does the complex of calmodulin with a peptide, C20W, derived from the calmodulin-binding domain of the Ca^{2+} pump of human erythrocytes (*58*).

In the TnC/TnI_{1-47} complex, the latter adopts an α-helical structure over 31 residues of its sequence (*42*). While the C-terminal 21 residues form a dense network of hydrogen bonds and hydrophobic interactions with the C-terminal lobe of TnC, the preceding 10 residues make only a small number of interactions with the N-lobe of TnC (Figure 6c). The authors suggest that the second set of contacts serves only to anchor the N-lobe to TnI but that these "do not play an essential role in recognition". In the complex formed between EF34 and ZR7, an α-helix is formed by ZR7 that is only slightly shorter than the portion of TnI_{1-47} that is in contact with the C-lobe of TnC. The extra turn of α-helix in TnI_{1-47} is stabilized by additional contacts of Arg14 with the N-lobe, while the corresponding lobe is absent in the EF34-ZR7 complex. Only the C-terminal 73 amino acids of α-actinin (EF34) are required for binding to ZR7 while the preceding two EF-hands have little effect on binding to ZR7 (*14*). Nonetheless, additional contacts might stabilize a slightly longer α-helix. Inspection of the model of the EF34-ZR7 complex (Figure 6d) suggests that Lys8 and Lys9 of ZR7 may play a similar role to Arg13 and Arg14 of TnI_{1-47} in forming contacts with N- and C-lobes and that Val16 could replace Met21 in making hydrophobic contacts important for recognition (*42*).

The three-dimensional structure of the complex formed by calmodulin with C20W reveals a mode of binding that is only slightly different to that of TnC to TnI_{1-47} (*59*). The peptide interacts solely with the C-lobe of calmodulin, almost perpendicular to the axis of the dumbbell, on the opposite face to that facing the N-lobe. The orientation of C20W with respect to the C-lobe is, however, highly similar to that of TnI_{1-47} on TnC, with the peptide lying across the same face of the lobe, at a slightly different angle. In the TnC-TnI_{1-47} complex, the peptide makes a few additional contacts with the N-lobe of TnC, whose orientation with respect to the C-lobe is quite different to that in calmodulin, forming a more compact, less extended structure. In both complexes the residue corresponding to EF34 Phe14 (Phe99) is surrounded by hydrophobic side-chains of the peptide. These complexes and the qualitative model of EF34 with ZR7 would appear to represent a general alternative binding mode of calmodulin-like domains to target peptides.

An additional α-actinin−titin interaction was described, between the two central spectrin-like domains of α-actinin and a 70-amino acid segment C-terminal to the last Z-repeat of titin (*18*). This is thought to account for co-localization of α-actinin with titin during myofibrillogenesis, even when the C-terminal EF-hand domains are deleted (*60*), and to provide a mechanism for delimiting the structure of the Z-disk (*18*). With this information and the detection of binding to all Z-repeats, Young et al. (*18*) proposed a model for the structure of the Z-disk, consistent with biochemical and biophysical data available to date.

How well do the structural data for the EF34-ZR7 complex agree with the proposed structure of the Z-disk (*18*)? The authors note that "orthogonally arranged pairs of Z-filaments are spaced by 15−20 nm" (*61*, *62*) and that "the interactions of titin Z-repeats and successive pairs of α-actinin molecules must roughly allow for this spacing". The experimental observation of pairs of Z-filaments requires that there be at

least two titin molecules per actin filament in the Z-disk, providing two equivalent sites at points along the filament. A fully extended Z-repeat could account for the observed spacing. According to our results, however, a stretch of 18 residues is in an α-helical conformation, which, if regular with a translation along the helix axis of 1.5 Å (*63*), is expected to have a length of 25.5 Å or 2.55 nm. Taking an average number of residues per Z-repeat of 46 (*19*) and a maximal displacement for an extended peptide chain of 3.47 Å per residue (*63*), the remaining 28 residues could span 97.2 Å (9.72 nm), giving a maximal length of the Z-repeat of 122.7 Å (12.27 nm). A less than extended structure for the nonhelical segment may more reasonably be supposed (the presence of proline residues alone suggests this), with two such repeats possibly being required to cover the 15−20 nm between the Z-filaments. Such a model would leave alternate Z-repeats empty although the number of Z-filaments observed experimentally (*60*, *61*) correlates well with the total number of Z-repeats.

While a number of domains along the length of titin have been characterized (*20*−*25*), this is the first structural study of the interaction of titin with another component of the sarcomere. Much remains to be done before the role of titin in organizing and regulating the sarcomere is fully understood.

ACKNOWLEDGMENT

The authors thank Drs. M. Gautel, S. Labeit, and P. Luther for helpful discussions, Dr. R. R. Biekofsky for critical comments on the manuscript, Drs. T. Frenkiel, M. Gradwell, and F. Muskett of the MRC NMR Centre for their advice and assistance in setting up NMR experiments, and Prof. C. Griesinger for providing the coordinates of the calmodulin/C20W complex prior to their release.

REFERENCES

1. Maruyama, K., Matsubara, S., Nonomura, Y., Kimura, S., Ohashi, K., Murakami, F., Handa, S., and Eguchi, G. (1977) *J. Biochem. 82*, 317−337.
2. Wang, K., McClure, J., and Tu, A. (1979) *Proc. Natl. Acad. Sci. U.S.A. 76*, 3698−3702.
3. Maruyama, K. (1994) *Biophys. Chem. 50*, 73−85.
4. Trinick, J. (1994) *Trends Biochem. Sci. 19*, 405−409.
5. Keller, T. C. S., III (1995) *Curr. Opin. Cell Biol. 7*, 32−38.
6. Trinick, J. (1996) *Curr. Biol. 6*, 258−260.
7. Maruyama, K. (1997) *FASEB J. 11*, 341−145.
8. Whiting, A., Wardale, J., and Trinick, J. (1989) *J. Mol. Biol. 205*, 263−268.
9. Labeit, S., Barlow, D. P., Gautel, M., Gibson, T., Holt, J., Hsieh, C.-L., Francke, U., Leonard, K., Wardale, J., Whiting, A., and Trinick, J. (1990) *Nature 345*, 273−276.
10. Labeit, S., and Kolmerer, B. (1995) *Science 270*, 293−296.
11. Eilertsen, K. J., Kazmierski, S. T., and Keller, T. C. S., III (1997) *Eur. J. Cell Biol. 74*, 361−364.
12. Machado, C., Sunkel, C. E., and Andrew, D. J. (1998) *J. Cell Biol. 141*, 321−333.
13. Ohtsuka, H., Yajima, H., Maruyama, K., and Kimura, S. (1997) *FEBS Lett. 401*, 65−67.
14. Ohtsuka, H., Yajima, H., Maruyama, K., and Kimura, S. (1997) *Biochem. Biophys. Res. Commun. 235*, 1−3.
15. Sorimachi, H., Freiburg, A., Kolmerer, B., Ishiura, S., Stier, G., Gregorio, C. C., Labeit, D., Linke, W. A., Suzuki, K., and Labeit, S. (1997) *J. Mol. Biol. 270*, 688−695.
16. Beggs, A. H., Byers, T. J., Knoll, J. H. M., Boyce, F. M., Bruns, G. A. P., and Kunkel, L. M. (1992) *J. Biol. Chem. 267*, 9281−9288.
17. Littlefield, R., and Fowler, V. M. (1998) *Annu. Rev. Cell Dev. Biol. 14*, 487−525.
18. Young, P., Ferguson, C., Bañuelos, S., and Gautel, M. (1998) *EMBO J. 17*, 1614−1624.
19. Gautel, M., Goulding, D., Bullard, B., Weber, K., and Fürst, D. O. (1996) *J. Cell Sci. 109*, 2747−2754.
20. Pfuhl, M., and Pastore, A. (1995) *Structure 3*, 391−401.
21. Improta, S., Politou, A. S., and Pastore, A. (1996) *Structure 4*, 323−337.
22. Politou, A. S., Gautel, M., Improta, S., Vangelista, L., and Pastore, A. (1996) *J. Mol. Biol. 255*, 604−616.
23. Pfuhl, M., Improta, S., Politou, A. S., and Pastore, A. (1997) *J. Mol. Biol. 265*, 242−256.
24. Improta, S., Krueger, J. K., Gautel, M., Atkinson, R. A., Lefèvre, J.-F., Moulton, S., Trewhella, J., and Pastore, A. (1998) *J. Mol. Biol. 284*, 761−777.
25. Muhle-Goll, C., Pastore, A., and Nilges, M. (1998) *Structure 6*, 1291−1302.
26. Ikura, M., Clore, G. M., Gronenborn, A. M., Zhu, G., Klee, C. B., and Bax, A. (1992) *Science 256*, 632−638.
27. McKay, R. T., Pearlstone, J. R., Corson, D. C., Gagné, S. M., Smillie, L. B., and Sykes, B. D. (1998) *Biochemistry 37*, 12419−12430.
28. Jeener, J. Meier, B. H., Bachmann, P., and Ernst, R. R. (1979) *J. Chem. Phys. 71*, 4546−4553.
29. Braunschweiler, L., and Ernst, R. R. (1983) *J. Magn. Reson. 53*, 521−528.
30. Bax, A., and Davis, D. G. (1985) *J. Magn. Reson. 65*, 355−360.
31. Piotto, M., Saudek, V., and Sklenár, V. (1992) *J. Biomol. NMR 2*, 661−665.
32. Sklenár, V., Piotto, M., Leppik, R., and Saudek, V. (1993) *J. Magn. Reson. Series A 102*, 241−245.
33. Bodenhausen, G., and Ruben, D. J. (1980) *Chem. Phys. Lett. 69*, 185−189.
34. Shaka, A. J., Barker, P. B., and Freeman, R. (1985) *J. Magn. Reson. 64*, 547−552.
35. Marion, D., Driscoll, P. C., Kay, L. E., Wingfield, P. T., Bax, A., Gronenborn, A. M., and Clore, G. M. (1989) *Biochemistry 28*, 6150−6156.
36. Zuiderweg, E. R., and Fesik, S. W. (1989) *Biochemistry 28*, 2387−2391.
37. Vuister, G. W., and Bax, A. (1993) *J. Am. Chem. Soc. 115*, 7772−7777.
38. Delaglio, F., Grzesiek, S., Vuister, G., Zhu, G., Pfeifer, J., and Bax, A. (1995) *J. Biomol. NMR 6*, 277−293.
39. Bartels, C., Xia, T.-H., Billeter, M., Güntert, P., and Wüthrich, K. (1995) *J. Biomol. NMR 5*, 1−10.
40. Vriend, G. (1990) *J. Mol. Graph. 8*, 52−56.
41. Vassylyev, D. G., Takeda, S., Wakatsuki, S., Maeda, K., and Maeda, Y. (1998) *Proc. Natl. Acad. Sci. U.S.A. 95*, 4847−4852.
42. Muñoz, V., and Serrano, L. (1997) *Biopolymers 41*, 495−509.
43. Meador, W. E., Means, A. R., and Quiocho, F. A. (1992) *Science 257*, 1251−1255.
44. Rhoads, A. R., and Friedberg, F. (1997) *FASEB J. 11*, 331−340.
45. Zappacosta, F., Pessi, A., Bianchi, E., Venturini, S., Sollazzo, M., Tramontano, A., Marino, G., and Pucci, P. (1996) *Protein Sci. 5*, 802−813.
46. Orrù, S., Dal Piaz, F., Casbarra, A., Biasiol, G., De Francesco, R., Steinkühler, C., and Pucci, P. (1999) *Protein Sci. 8*, 1445−1454.
47. Scaloni, A., Miraglia, N., Orrù, S., Amodeo, P., Motta, A., Marino, G., and Pucci, P. (1998) *J. Mol. Biol. 277*, 945−958.
48. Scaloni, A., Monti, M., Acquaviva, R., Tell, G., Damante, G., Formisano, S., and Pucci, P. (1999) *Biochemistry 38*, 64−72.
49. Travé, G., Pastore, A., Hyvönen, M., and Saraste, M. (1995) *Eur. J. Biochem. 227*, 35−42.
50. Tokuyasu, K. T., and Maher, P. A. (1987) *J. Cell Biol. 105*, 2781−2793.
51. Fürst, D. O., Osborn, M., and Weber, K. (1989) *J. Cell Biol. 109*, 517−527.

52. Finn, B. E., and Forsén, S. (1995) *Structure 3*, 7−11.
53. James, P., Vorherr, T., and Carafoli, E. (1995) *Trends Biochem. Sci. 20*, 38−42.
54. Farah, C. S., and Reinach, F. C., (1995) *FASEB J. 9*, 755−767.
55. Perry, S. V. (1999) *Mol. Cell. Biochem. 190*, 9−32.
56. Trewhella, J., Blumenthal, D. K., Rokop, S. E., and Seeger, P. A. (1991) *Biochemistry 29*, 9316−9324.
57. Kataoka, M., Head, J. F., Vorherr, T., Krebs, J., and Carafoli, E. (1991) *Biochemistry 30*, 6247−6251.
58. Elshorst, B., Hennig, M., Försterling, H., Diener, A., Maurer, M., Schulte, P., Schwalbe, H., Griesinger, C., Krebs, J., Schmid, H., Vorherr, T., and Carafoli, E. (1999) *Biochemistry 38*, 12320−12332.
59. Schultheiss, T., Choi, J., Lin, Z. X., DiLullo, C., Cohen-Gould, L., Fischman, D., and Holtzer, H. (1992) *Proc. Natl. Acad. Sci. U.S.A. 89*, 9282−9286.
60. Luther, P. K. (1991) *J. Cell Biol. 113*, 1043−1055.
61. Schroeter, J. P., Bretaudiere, J. P., Sass, R. L., and Goldstein, M. A. (1996) *J. Cell Biol. 133*, 571−583.
62. Cantor, C. R., and Schimmel, P. R. (1980) *Biophysical Chemistry. Part I: The Conformation of biological macromolecules*, W. H. Freeman and Co., New York.
63. Wishart, D. S., Sykes, B. D., and Richards, F. M. (1991) *J. Mol. Biol. 222*, 331−333.
64. Merutka, G., Dyson, H. J., and Wright, P. E. (1995) *J. Biomol. NMR 5*, 14−24.
65. Thompson, J. D., Gibson, T. J., Plewniak, F., Jeanmougin F., and Higgins, D. G. (1997) *Nucleic Acids Res. 25*, 4876−4882.

BI991891U